Master's thesis in Urban and Regional Planning

Effect of Urbanization on surface urban heat island（SUHI）in North District of Hong Kong, using remote sensing techniques

August 2023

Seoul National University

Graduate school of environmental studies

Urban and Regional Planning

ZHANG HENG

Effect of Urbanization on surface urban heat island（SUHI）in North District of Hong Kong, using remote sensing techniques

Advisor：Young-Sung LEE

Submitting a master's thesis of Urban and Regional Planning

August 2023

Graduate School of Environmental studies

Seoul National University

Urban Regional Planning
ZHANG HENG

Confirming the master's thesis written by

ZHANG HENG

August 2023

Chair **Steven Jige QUAN** (Seal)

Vice Chair **Jae-Min SONG** (Seal)

Examiner **Young-Sung LEE** (Seal)

Abstract

There is direct relationship between urbanization and Land use and cover (LULC) change, there is also relationship between the land surface temperature (LST) and Albedo, Albedo and LST can be influenced by urbanization at the same time. In this study, I try to explore the impact of urbanization on surface urban heat island (SUHI). There is no research studied by remote sensing method in North District of Hong Kong. In this study, i have classified the LULC in North District of Hong Kong, then, LST has been analyzed by using Landsat (TM/OLI) images. The inversion LST was obtained in this study's usage of the maximum likelihood classifier approach (supervised classification) to categorize pictures. There are so many methods to define urban area and non-urban area, simplified urban extend (SUE) method is used to distinguish urban area and non-urban area and then calculate the surface urban heat island (SUHI) in North District of Hong Kong, the correlation between urban heat island effect and urban green space and building land can provide important information for our urban development and environmental protection. To study the influence of urban green space and building land on urban heat island effect, I also analyzed the correlation between land surface temperature and Albedo, and the relationship between LST and NDVI, NDBI shows the influence of vegetation area on UHI is negative. Then the positive correlation between urban building land and surface temperature distribution is that urban building land has a positive influence on UHI, it also shows building area can enhance urban heat island effect. The results of LULC revealed that According to the classification results, from 1987 to 2004, 71.157% of forest area remained unchanged, 26.903% of forest was changed into urban area, and 9.529% of barren was changed into urban area. From 2004 to 2021, 71.157% of forest area remained unchanged, 26.903% of forest area was changed into urban area, 9.529% of barren area were changed into urban area. From 1987 to 2021, 42.654% of forest area changed into another land area, urban area continued to increase from 1987 to 2021.

Keywords: Land surface temperature (LST), Urbanization, Albedo, Surface urban heat island (SUHI).

CONTENTS

CHAPTER I. INTRODUCTION

1.Research Objectives and Significance of Study

The severity of the Urban Heat Island Effect continues to increase because of the vast urban population, urbanization, changes in the underlying surface, canopy structure, and artificial heat exhaust.

The impact of the UHI is receiving unprecedented attention. The urban heat island effect can not only affect people's regular work and life but also influence their overall well-being. Urban climate and environment have also developed rapidly with the continuous improvement of urbanization. During urbanization, many people are moving into cities from all directions, leading to increased industrial production that consumes a lot of non-renewable energy. Simultaneously, there are more artificial heat emissions from automobile exhaust gas, industrial exhaust gas, and other sources. As a result, the average temperature of the entire city keeps rising.

On the other hand, the influx of population requires a larger construction area, resulting in changes to the city's underlying surface. Cement, asphalt, and other artificial impermeable surfaces are expanding, while vegetation coverage is decreasing. This leads to a change in the thermal properties of the city's underlying surface, making it more heat-absorbing and less reflective than natural vegetation, thus causing higher average temperatures throughout the city. Due to a phenomenon known as the "urban heat island effect," metropolitan regions often experience much warmer average temperatures than suburban areas. As urbanization progresses and the urban underlying surface changes, the intensity and distribution characteristics of the urban heat island effect will also change significantly. With rapid urbanization and the expansion of urban areas, the high-temperature areas become more extensive, therefore the urban heat island effect will be more widely distributed. The increasing average urban temperature will raise the energy consumption of refrigeration equipment and the electricity burden of the whole city.

Hong Kong is now grappling with a serious urban heat island (UHI) problem. However, all research mentioned so far focuses on the most severe UHI issue in the North district of Hong Kong, there is no separate research referring to urban heat islands in this district. Hence, in this study, we will explore the effect of urbanization on surface urban heat islands in the North district of Hong Kong using remote sensing methods. Since the late 20th century, with the advent of high-resolution Earth exploration satellites, remote sensing techniques to detect land surface temperature (LST) and study the urban heat island effect have become popular. There are many benefits to using remote sensing to study the urban heat island effect, including high resolution, comprehensive coverage, and point density, which mitigate for the inadequacies of conventional meteorological observation techniques and enable the study of the urban heat island effect in wide-ranging regions.

Landsat TM data is often the most excellent option for researching the urban heat island effect due to its high thermal resolution. In this study, I used Landsat TM images from 1987, 2004, and 2021 as data sources to analyze the thermal band and retrieve the surface temperature of North district of Hong Kong over the past 20 years. Using the maximum likelihood method, the ENVI 5.3 software has been used for the supervised classification of remote sensing images, and the

Confusion matrix has been utilized to assess the precision of classification outcomes. The kappa coefficient and total accuracy are anticipated to be higher than 90%. LULC images have been classified into four classes: urban area, water area, forest area, and barren area, after which we can examine how the land surface temperature is spatially distributed among these various land classes. In the North district of Hong Kong, the urban area has expanded from 1987 to 2021, while the forest area and barren area have decreased. It indicated that the urban surface temperature was the greatest, followed by that of the barren area, while the forest area was the lowest temperature. Then, I have calculated the surface urban heat island intensity (SUHI), and it revealed that the surface urban heat island intensity has increased from 1987 to 2021. Finally, i conducted a correlation analysis between LST and EDVI, NDBI, to obtain the correlation trend between LST distribution and urban area and forest area. The outcome may be used as a basis for rational urban planning, urban development, and decision-support to improve the quality of life in Hong Kong's North area.

2. The influencing factors of Urban Heat Island.

Many academics have disclosed the link between urban heat island from many viewpoints, such as the influence of diverse land cover and land use (LULC) types on urban heat island at various times of the day and night, as well as throughout the seasons. Heinl, Singh, and colleagues studied the intensity and geographical distribution of urban heat islands. The findings reveal that the number of impermeable surfaces is directly connected to the severity of the urban heat island. Cheval, Alves, and colleagues investigated the intensity and geographical distribution of urban heat islands under various seasonal circumstances. The parameters of the urban heat island changed according to the season. Krehbiel et al. did research to compare urban heat island during the day and night, and discovered that the urban heat island impact is considerable both during the day and at night. Vallati investigated the effect of urban heat islands on the energy consumption of urban structures in Rome, Italy. According to the findings, cooling demand for urban structures grew by 33% in the summer but declined in the winter. Gu discovered that the link between climate, precipitation, and urban heat island varies depending on the season. The severity of the urban heat island is favorably connected with precipitation in the summer, while it is more evident in the winter. There is no significant correlation between rainfall and temperature. Moon explored the mitigation effect of urban heat island by using various greening patterns for urban buildings, including exterior greening, interior greening, and roof greening.

3. Research Range

The Hong Kong Special Administrative Region, sometimes known as "Hong Kong," is a part of southern China that is situated to the east of the Pearl River estuary and across the sea from the Chinese cities of Macao, Shenzhen, and Zhuhai. With a population of 7,333,200 in 2020, it is one of the world's most densely inhabited areas, with the highest human development index and life expectancy. Since ancient times, Hong Kong has been a part of China. From 1842 to 1997, it was governed by the British. Being one of the "Four Little Dragons of Asia" and a region with one of the wealthiest, most developed economies, and the best living standards worldwide, Hong Kong's economy and society evolved rapidly after the Second World War, On July 1, 1997, Hong Kong was handed over to the Chinese government. Hong Kong, which has long maintained a capitalist economy and enjoys considerable autonomy in other areas except for foreign and defense issues, is entirely under the supervision of the Central Government. The core tenets of the Chinese government's national policy are "one country, two systems," and a high level of autonomy. Alongside New York and London, Hong Kong is one of the three Harbor cities—a thriving free port and a global metropolis. It is a crucial hub for global commerce, shipping, innovation, and technology and the third-largest financial center in the world. The traditions of China and the West are blended in Hong Kong, combining Chinese managerial expertise with Western knowledge, and it is regarded as having a competent legal system, a free market, and a government that operates with integrity.

Due to the low latitude and close to the sea, there is a subtropical Marine monsoon climate in Hong Kong, characterized by neither hot summer nor cold winter. Also due to the geographical location of the southeast coast of the Asian continent, deeply affected by the monsoon, the formation of the mid-year weather seasonal changes are significant characteristics. Hong Kong's climate has four different seasons due to the cooling impact of the mainland in winter and the urban heat island effect of the mainland in summer, and the climate difference is large. Therefore, there is hot in summer and sudden cooling in winter. At the same time, due to the influence of tropical and temperate weather, Hong Kong's weather has different changes from day to day. The high degree of development in Hong Kong raises serious concerns about the urban heat island effect. In the North district of Hong Kong, the urban heat island issue is not much more severe than in other regions of Hong Kong. However, over time, the impact of urbanization on the urban heat island becomes increasingly problematic.

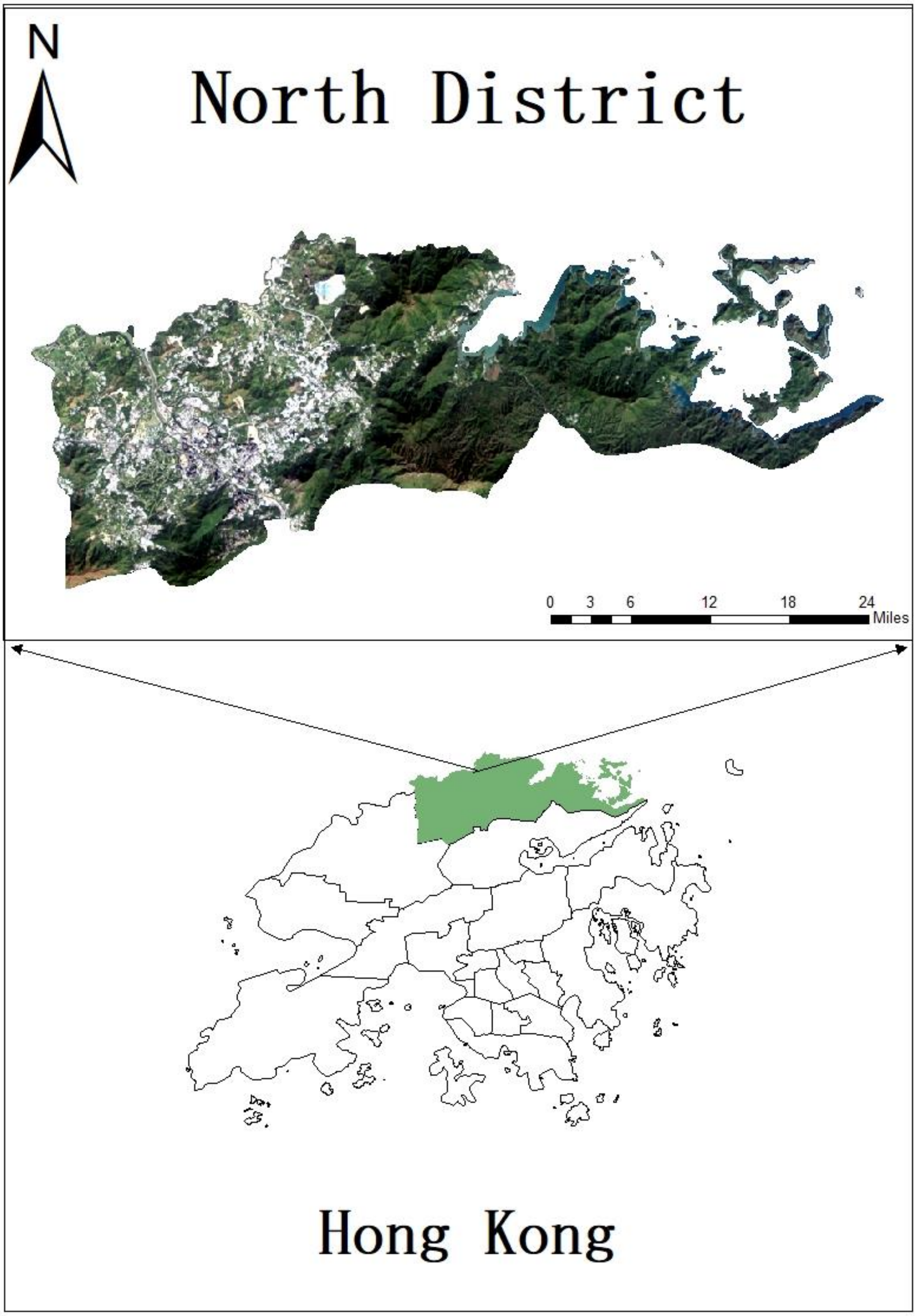

Figure 1: Location of North district of Hong Kong

4. Problems among studies

The research methods for studying urban heat island include the establishment of ground meteorological observatories, utilization of mathematical models, analysis of remote sensing data, and application of landscape ecology theory. However, there are still areas that need improvement in the research process. Most of the studies mentioned above focus on big cities or mega-cities, such as Beijing, Shanghai, London, and other large-scale urban areas. When it comes to the analysis of remote sensing data method, there are also many problems among studies, first, the impact of weather, second, Land surface information loss, the accuracy is not that high.

CHAPTER II. LITERATURE REVIEW

1. Urban heat island (UHI) and urban heat intensity (UHII)

Typically, a city's atmospheric temperature is significantly higher than that of the adjacent suburbs due to the urban heat island effect. The urban high-temperature zone is called an "urban heat island" because it seems to be an island sticking out of the water on the temperature map, even though the temperature difference in the suburbs is minimal on the near-surface temperature map. "Urban heat island intensity (UHII)" refers to the difference between the greatest temperature in suburban areas and the highest temperature in urban areas, as defined by Oke in 1987.

After comparing temperatures in urban and suburban London, in 1833, Lake Howard, a British climatologist, postulated the "urban heat island effect" in Climatology published in London. This marks the first time that "the ban heat island effect" has been documented. In 1958, Manley introduced the Urban Heat Island (UHI).

When it comes to urbanization, it is used to describe two processes that are different but related to each other. On the one hand, it relates to the absolute and relative proportion of individuals residing in densely populated areas who engage in non-agricultural activities. On the other hand, it involves transforming the natural landscape (e.g., the LULC change) into an environment that is suited for human habitation.

A phenomenon known as the urban heat island (UHI) is defined by the temperature disparity between metropolitan areas (or portions of them) and the surrounding non-urban areas. This difference assumes that the natural environment would have a different temperature if urbanization did not exist. Urban heat islands may be divided into four categories:

1. Canopy-level urban heat island (CUHI): This refers to the near-surface air temperature below the height of roofs in urban areas.
2. Boundary-level urban heat island (BUHI): This is calculated using the air temperature above the height of buildings.
3. Surface urban heat island (SUHI): This is determined by the temperature of the three-dimensional urban surface, including the ground, walls, and rooftops.
4. Substrate urban heat island (GUHI): This considers the temperature of the soil beneath the ground surface.

This study primarily focuses on the surface urban heat island (SUHI). The SUHI effect occurs when the complex urban structure, with its buildings and infrastructure, traps and retains heat, leading to temperature variations at a microscale. Solar energy absorption and distribution on the urban surface play a significant role in this process, affecting the local temperature. Additionally, various human activities, such as vehicle emissions, building heating, and industrial processes, contribute to the SUHI effect.

2. The research methods of urban heat island and progress

There are currently three primary approaches to studying urban heat island, 1. surface meteorological data observation between urban areas and suburban areas, 2. remote sensing monitoring, 3. boundary layer numerical model simulation. The approach for observing ground-surface meteorological data is based on sparse data from stationary meteorological stations in suburbs, combined with flow observation data to make a comparative observation of temperature and surface temperature. Remote sensing monitoring uses aerospace sensors to observe the urban underlying surface temperature. Boundary layer model simulation employs mesoscale models from one to three dimensions to simulate the temperature, humidity, and wind fields at a specific height.

3. Surface meteorological data observation between urban area and suburb area

The Comparison Method of Peri-urban Meteorological Observation Data is the first approach used to study the Urban Heat Island effect. This method utilizes multi-year observations from meteorological stations in both urban and suburban areas. The data is subjected to comparative analysis using statistical or mathematical simulations to analyze the distribution and intensity of the urban heat island during the same period, as well as its variation throughout the day and season. Since the early days of research, the average temperature in the metropolis was 1.1 degrees Celsius higher than in the suburbs, according to Howard. Duckworth and Sandberg later supported this finding. In the case of San Francisco, a temperature difference of 10°C was observed between the park and the City Centre, showing similarities to Howard's results. Consequently, the study concludes that the urban heat island effect in most cities is more severe during winter than in summer, and this seasonal variation is evident. Additionally, wind speed is identified as the primary factor determining urban heat island. As wind speed increases, the temperature difference decreases, while the urban heat island effect becomes more pronounced with the city size. Zhou Shuzhen et al. were the first group to discover the urban heat island effect in Shanghai, observing a significant temperature difference of 5°C higher than in suburban areas, particularly 2-3 hours after sunset. This effect is more pronounced during the night. Over the years, data has revealed that the expansion of downtown Shanghai has widened the temperature difference in its suburbs, leading to an increase in annual minimum temperatures by 0.7°C in 1984.

3.1 Boundary layer numerical model simulation

The urban heat island effect is simulated by using statistical modules combined with an analog prediction method. This simulation involves the use of type, physical, numerical, and analytical models. Among these, the most widely applied model is the numerical simulation of the boundary layer, which employs the principles of thermodynamics and dynamics to examine the energy equilibrium and temperature field. By utilizing boundary layer numerical modeling, it is possible to study the energy balance, fundamental properties of the temperature field, and the heat transfer process between the ground and the atmosphere. The initial modeling of the urban heat island effect was conducted by Myrup using the most basic one-dimensional equation. In subsequent studies, Carlson and Artbus emphasized the importance of considering surface heat flow, and they simulated surface heat response processes with precise surface parameter selection. To obtain a spatial distribution model and understand the time and space-time evolution of the heat island, researchers have coupled boundary layer and remote sensing methods. Additionally, the "urban canyon" impact on the surface energy balance was first included by Oke et al. The Japanese Yoshikadao school uses three-dimensional modules to study the interplay between sea wind and heat island circulation in Tokyo.

3.2 Remote sensing monitoring

The research of the urban heat island effect has been profoundly affected by the growth and development of remote sensing technology. Compared to traditional methods, the remote sensing inversion method offers many advantages, such as comprehensive coverage, visual representation, and high synchronization in time. This method is based on analyzing the absorption of solar long-wave radiation characteristics by different objects, which results in varying radiation values in different wave segments. Thermal infrared sensors are used to observe the urban geological temperature.

The advent of remote sensing and satellite technologies in the 1980s enabled the investigation of the urban heat island effect by remote sensing monitoring. This monitoring method involves continuous and periodic observations of surface temperature using spaceborne or airborne sensors. Remote sensing data may be translated to absolute surface temperatures using Geographic Information Systems (GIS). The sensor data can then be interpreted and analyzed to provide corresponding surface cover data, considering the different absorption characteristics of solar radiation. Remote sensing monitoring methods allow for the collection of urban surface data over a wide range, providing synchronous and direct reflections of the spatial-temporal distribution of urban surface temperatures.

Currently, various data can be used for remote sensing monitoring, primarily including NASA Landsat series data such as Landsat TM/ETM+, Landsat OLI-TRIS, MODIS, ASTER, AVHRR, etc. [31] Different remote sensing data have distinct characteristics, Landsat series have higher resolution and easier to acquire. In contrast, MODIS and ASTER data offer shorter re-visit cycles and higher accuracy. As a result, while studying urban heat islands, the remote sensing data used must be adjusted to the unique demands of the research.

Scholars, such as Wei Lingling, Liu Bingbing, et al. have conducted studies on urban heat island in Nanjing, Changsha, Shanghai, and Beijing city based on remote sensing data. Hou Haoran et al. utilized remote sensing to study the spatial and temporal evolution of urban heat island in Fuzhou over the past 20 years. Chen Yunhao used remote sensing data to invert the surface temperature of Shanghai and analyzed the spatiotemporal characteristics of the city's overall thermal environment. Li Haifeng analyzed the urban heat island in Mianyang City by using remote sensing images and found no significant difference in intensity between urban heat island and non-urban heat island. Using MODIS surface temperature data and DMSP night light data, Wang Li investigated the spatial-temporal aspects of urban growth in China and its link with urban heat island.

Since Rao's first research on the urban heat island effect by utilizing satellite remote sensing in 1972, many scholars have extensively used sensor data from various platforms, including space, aviation, and ground data for urban heat island research. Qualitative remote sensing analysis involves studying the absorption of the sun's long-wave radiation by various geological features, resulting in different wavelength radiation values. This information is then used with thermal infrared sensors to observe urban geological temperature within a specific range, followed by calculation and interpretation using computer technology to analyze the heat distribution of the earth's objects. Differences in suburban vegetation status are also analyzed based on vegetation indices. To determine the approximate range of the urban heat island, the color synthesis of two different phases of TM (4-6 Band) is used against the target urban area. The effect of the urban heat island on temperature differences in suburban areas is estimated. Furthermore, remote sensing monitoring is commonly used for surface temperature analysis, which involves studying the absorption of long-wave radiation from the sun by different surface features. This process includes summarizing geographical conditions, climatic characteristics, and temperatures of the city, followed by image processing for grayscale stretching and density segmentation. Bright temperature data are obtained using the bright temperature calculation mode, and simultaneous geometric correction, calibration, mosaic, shear, and density segmentation are performed. Finally, the central distribution area and field structure characteristics of the heat field are analyzed. NOAA or Landsat TM images are used to determine the number of bright temperatures obtained. The flatness of the urban heat island effect in different seasons is also analyzed. This data is valuable for studying the distribution of urban areas, urban planning, urban environmental quality assessment, and environmental protection in cities. Ma Wai et al. studied Beijing's surface temperature using Landsat-5 data based on atmospheric adjustment, focusing on the impact of plant cover on surface temperature.

3.3 Temperature-Based Heat Island remote sensing Monitoring Method

Thermal infrared remote sensing records the emission radiation and rings of surface objects. Satellite brightness temperatures can conveniently replace the sum of ambient and atmospheric radiation. While satellite brightness temperature, ground temperature, and temperature are closely related to each other. Different temperature monitoring methods can be used according to the treatment temperature means. There are two sub-categories: brightness-based temperature monitoring and the surface-based monitoring temperature method. Research on Urban Heat Island Based on Bright temperature assumes that due to the limited area of the city, the water in the study area can be considered in a vapor state approximately the same. Therefore, the effect of the atmosphere on the radiant temperature can be disregarded. Many scholars used NOAA/AVHRR or Landsat Bright Temperature Data of TM/ETM Images.

However, surface heat radiation is exposed to the atmosphere and radiation surfaces during its conduction. There is a heavy impact on it, and the thermal radiation intensity observed by satellite remote sensing is no longer a simple surface thermal radiation intensity, bright temperature, and proper surface temperature. There is a significant difference, sometimes up to 5~6K. So, using bright temperature to proceed directly with Urban Heat Island research has excellent limitations. A Basic Study of Surface Temperature Monitoring Method in Inverting Temperature considers the multiple effects of the atmosphere and radiation surfaces, but due to the urban underlying surface's unusual complexity and the difficulty of obtaining real-time sounding data at transit times, it is challenging to overcome the precise inversion of surface temperature. Currently, monitoring methods based on surface temperature are generally obtained by several simplified methods, such as specific radiance and atmospheric parameters.

3.3.1 A Method of Heat Island Remote Sensing Monitoring based on Vegetation Index (NDVI)

In remote sensing applications, the vegetation index reflects surface vegetation and it’s the most important source of information widely used for qualitative and quantitative evaluation of valuable vegetation cover and its vitality. In 1993, for the first time, GALLO et al. estimated urban heat island by using vegetation index obtained from AVHRR data. The role of the urban heat island effect in causing differences in urban and rural temperatures results in a table-like surface radiation temperature between vegetation index and urban and rural temperature. There was also a clear linear relationship and explanation for the mean minimum temperature concerning spatial change.

Further research has shown that in this field, the NDVI difference between urban and rural regions is identical to the difference between those two locations. There is a relationship between the urban and rural surfaces' respective minimum temperature differences during the same period. The relationship between temperature and urban and rural minimum temperature differences should be closer and more stable. There may be a distinction between urban and rural regions because of the NDVI difference between the two. Surface differences in minimum temperature (urban heat island effect) in different environmental material attributes. However, the vegetation index-based monitoring side has several limitations to the law which cannot be ignored. The study only applies to regional cities, and the elevation difference between villages should not exceed 500m. Areas of colored vegetation are not applicable; ③ Cities in arid climates are not applicable.

3.3.2 A Method of Heat Island remote sensing Monitoring Based on "Heat Landscape."

A Monitoring Method Based on "Heat Landscape" by Chen Yunhao et al. which was conducted through the research method of landscape ecology and introduced the concept of "thermal landscape." It is considered studying from a landscape viewpoint by using GIS and remote sensing technologies, it’s a study on the Spatial Pattern and Process of Urban Thermal Environment. The evaluation index of the method is divided into fractal dimensions, number, shape index, dominance, fragmentation, separation, and diversity. This approach analyzed Shanghai's thermal environment's spatial pattern and dynamic development. The findings demonstrate that the thermal environment evolves in tandem with urban growth, becoming more fragmented and polished because of human activity.

4. Research urban heat island by remote sensing inversion

Up to now, the commonly used satellite thermal infrared remote sensing information sources are shown below.

Table 1: satellite thermal infrared remote sensing information sources

Frequently-used thermal infrared data sources for SUHI monitoring

PLATFORM / SENSOR	SPATIAL RESOLUTION	CYCLE/D	STARTING TIME	Thermal Band Number
GOES /GOES	4 km	~0 d	1974	dual band
FY-2/SVISSR	5 km	~0 d	2004	dual band
MSG /SEVIRI	3 km	~0 d	2005	dual band
NOAA /AVHRR	1.1 km	≤0.25 d	1979	dual band
Terra/MODIS	1 km	0.5 d	2000	dual band
Aqua/MODIS	1 km	0.5 d	2002	dual band
HJ-1B/IRS	300 m	4 d	2008	single band
FY-3/MERSI	250 m	5.5 d	2008	single band
Landsat/TM、ETM+、TIRS	60~120 m	16 d	1982	dual / single
Terra/ASTER	90 m	15 d	1999	single band
CBERS/IRMSS、IRS	80~156 m	26 d	1999	dual band
Sentinel 1,2/MSI	10m, 20m, 60m	5 d, 10 d	2015	dual band

Numerous surface temperature inversion approaches, such as the conventional radiation transfer equation method, the split window algorithm (1996), the single window algorithm (2001), etc., have been presented based on various remote sensing image data. The radiation transfer equation approach initially requires an atmospheric simulation to deduct the quantity of radiation from the thermal radiation measured at satellite height to get the real thermal infrared radiation.

4.1 Radiation transfer equation method

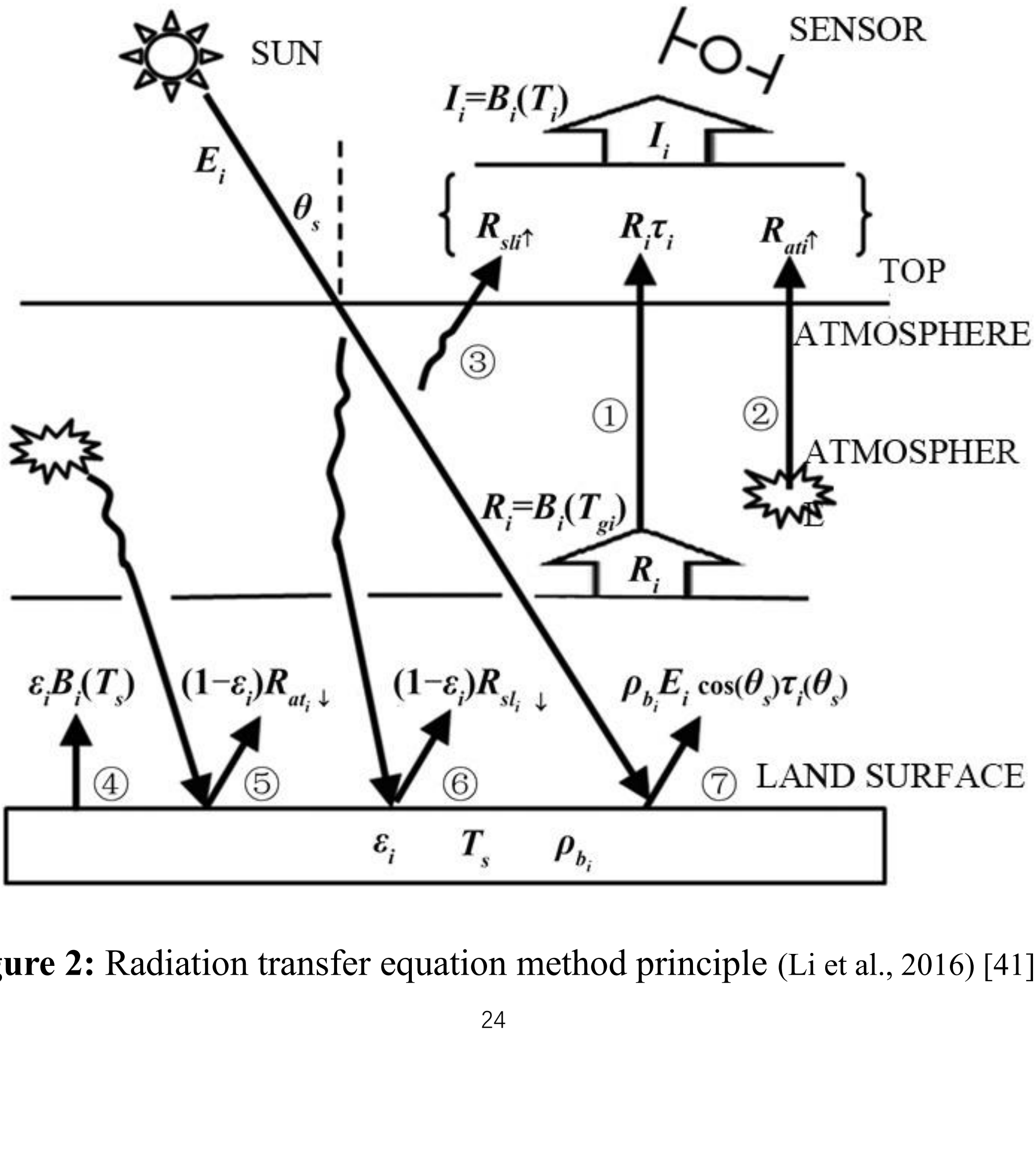

Figure 2: Radiation transfer equation method principle (Li et al., 2016) [41]

The effects of the atmosphere on surface thermal radiation are first evaluated by using a technique based on the radiation transport equation. The thermal infrared radiance value Lλ that the satellite sensor measures comprise three components: atmospheric radiance L↑, actual radiance on the ground detected by the satellite sensor after traveling through the atmosphere, and atmospheric radiance. The following is an example of a radiation transfer equation:

$$L_{\lambda} = [\varepsilon B(T_S) + (1-\varepsilon)\, L\downarrow]\, \tau + L\uparrow \tag{1}$$

Where ε denotes the surface's particular emissivity, TS denotes the temperature of the surface in Kelvin, B (TS) is the brightness of the blackbody thermal emissivity, and τ denotes the atmosphere's thermal infrared band transmittance. The thermal infrared band's thermally heated black body's radiant brightness B (TS).

$$B(T_S) = [L_{\lambda} - L\uparrow - \tau(1-\varepsilon)\, L\downarrow]/\tau\varepsilon \tag{2}$$

From Planck's formula, Ts may be calculated.

$$TS = K2/\ln(K1/ B(TS)+ 1) \tag{3}$$

4.2 Mono-window algorithm

Qin Zhihao (2004) developed the Mono-window Algorithm, which inverts the surface temperature by using Landsat TM/ETM+ 6th band data. The algorithm's mathematical formula is as follows:

$$T_S = [a\,(1- C- D) +(b\,(1- C- D)+C+D)\, T_6- DT_a]/C \tag{4}$$

Where TS refers to the actual surface temperature (K), and a and b are constants (-67.355351 and 0.458606, respectively). C and D represent intermediate variables, where C = ετ, and D = (1-τ) * [1 + (1-ε) * τ]. Here, ε refers to the surface-specific emissivity, τ refers to the atmospheric transmittance, and T6 is the brightness temperature (K) of pixels detected by sensors at satellite altitude.

4.3 Split-window algorithm

Split-window algorithms were created to invert sea surface temperatures first, notably for NOAA/AVHRR channels 4 and 5. They have subsequently been used to invert surface temperatures. The split window algorithm adjusts the ratio of the brightness of the atmosphere and the surface using two neighboring thermal infrared channels (10.511.5m and 11.512.5m) in the atmosphere window. This phrase is used:

$$T_S = T_4 + A(T_4 - T_5) + B \tag{5}$$

T4 and T5 are the AVHRR's channels 4 and 5, respectively, while TS is the real surface temperature, and A and B are constants. Channel 4(10.15~11.13μm) and channel 5 (11.15~12.15μm) of AVHRR correspond to the center wavelength of 31st wavelength of MODIS (10.178~11.128μm) and 32nd wavelength (11.177~12.127μm) of MODIS.

5. The effect of urbanization on urban heat island by remote sensing

When studying surface urban heat island, remote sensing techniques are typically used to examine how surface temperature and urban heat island intensity (UHII) fluctuate over time. For example, (Muhammad et al., August 15, 2022) selected three remote sensing images from different years. They calculated the average temperature and urban heat island intensity (UHII) for each of these remote sensing images for the same month. Next, they obtained land use/land cover (LULC) classification outcomes for each remote sensing image and compared the LULC images with temperature distributions. Finally, they investigated the connection between urbanization and urban heat island.

.

CHAPTER III. RESEARCH METHODOLOGY

1. Research Contents and Technical Route

1.1. Research Contents

After analyzing the above methods, this study adopted the remote sensing monitoring technique to evaluate the urbanization process of the North district of Hong Kong. This research looks on the relationship between urban surface Land use and Land cover (LULC) and the urban heat island, examined the characteristics of urban landscape patterns and the impact of urban heat island. This research suggests strategies to reduce the urban heat island impact and urban heat island intensity based on the geographical and temporal development and distribution of the urban heat island in Hong Kong's North district.

Firstly, three Landsat datasets from 1987 to 2021 of the North districts of Hong Kong were obtained from the geospatial data cloud. The data were carefully chosen to be as close in time as possible and accurate. After pretreatment on the ENVI 5.3 platform, 3 sets of surface temperature inversions were obtained by using the radiation transfer equation algorithm, and the surface temperature distribution characteristics were analyzed at different time points.

Based on the Landsat data, the Land Use and Land Cover (LULC) images of the North district of Hong Kong in 3 different years were derived by using the maximum likelihood classification method. After classification, the changes in urban surface within the North district of Hong Kong were analyzed. NDVI and NDBI were calculated, and the correlation between NDVI and NDBI was studied through linear regression.

By using satellite thermal bands, I estimated the land surface temperature of North district of Hong Kong using Landsat data to categorize land use and land cover (LULC). The years 1987, 2004, 2021, and December were all covered by the Landsat data collection. Before classifying a picture, ENVI 5.3 was used for radiometric calibration, adjustments for air conditions, and calculating LST using the thermal band. The Maximum Likelihood Classifier Algorithm in ENVI 5.3 was used to conduct LULC classification, and accuracy was evaluated using fieldwork and randomly selected Google Earth sites.

Table 2: In this investigation, satellite pictures were employed.

Data source	Time	Spacial resulution (m)	Path/Row	Description
Landsat 5 TM	08 Dec. 1987 ,12;22 UTC+8	30	115/37	Geospatial Data Cloud
Landsat 5 TM	06 Dec. 2004 ,12;37 UTC+8	30	115/37	Geospatial Data Cloud
Landsat 8 OLI	05 Dec. 2021 ,12;52 UTC+8	30	115/37	Geospatial Data Cloud

1.2. Technical Route

Firstly, the pre-processiof to remote sensing data should be conducted. The exponential and ratio methods were employed to invert the land surface temperature and analyze the urban heat island's evolution process and distribution characteristics. Then, the maximum likelihood classification method was applied to classify land use and land cover (LULC) on the surface, and the land use and land cover (LULC) status was analyzed, including land use and land cover change, the distribution of land surface temperature (LST), and the study on the influence of different LULC types on the urban heat island. Using the outcomes of the categorization of land use and land cover, the Land Surface Temperature (LST), Surface Urban Heat Island (SUHI), and Urban Heat Island Intensity (UHII) are analyzed. On the other hand, the change of albedo was also analyzed at the same time, then, the association between urbanization and urban heat island is revealed in this study.

1.2.1. Access to remote sensing data

Landsat series, developed and launched by NASA in 1972, is a satellite engineering program designed for various applications in agriculture, mapping, forestry, regional planning, monitoring, and education. Since its inception in 1972, Landsat Data has deployed eight satellites equipped with sensors that transmit millions of image data for research in diverse fields. Among these satellites, Landsat 7, launched in 1999, is the seventh one and carries an enhanced thematic mapper that increases the panchromatic band resolution to 15 m and improves the data resolution of band six from 120 m to 60 m. The 2013 launch of Landsat 8, the newest satellite, will be accompanied by the newest Land Imager (OLI) and Thermal Infrared Sensor (TIRS), further enhancing its resolution compared to Landsat 7. Even though Landsat 1 to 5 are retired, they are still operational and contribute to the missions of Landsat 7 and 8. For this study, three Landsat images of 1987 (Landsat 5 TM), 2004 (Landsat 5 TM), and 2021 (Landsat 8 OLI) are selected as data sources. These images are clear, cloud-free (< 5%), and can provide a comprehensive view of the research area.

1.2.2. Remote sensing data preprocessing

Before this research, the dataset should be conducted through Geometric distortion, atmospheric extinction, and radiation distortion exist to remote sensing images, degrading not only their quality but also impacting the accuracy of research results.

(1) Geometric correction

In addition to realizing the normal geometric correction function, the method can also eliminate geometric distortions caused by terrain fluctuations by measuring elevation points and DEM. Orthogonally corrected images have precise spatial positions.

(2) Atmospheric correction

Spaceborne sensors are influenced by the atmosphere and light, affecting the reflectance, emissivity, and surface temperature of natural objects. Atmospheric correction can eliminate these effects. There are various atmospheric correction methods for remote sensing images, which can be divided into absolute and relative atmospheric correction methods. I utilized ENVI 5.3, which incorporates various atmospheric correction models, the dark pixel technique, and the statistical model-based reflectance inversion method, and the MORTRAN model based on the radiation transmission model. The relative atmosphere correction methods include the invariant target and histogram statistics methods. I chose the FLAASH atmospheric correction tool of ENVI 5.3, developed based on the MODTRAN4+ radiation transmission model and belongs to the absolute atmospheric correction method.

(3) Radiometric calibration

Surface and brightness temperatures are not directly obtained from the onboard sensor recordings. The sensor records the shadow value of the ring element (DN), requiring a conversion to obtain the corresponding physical information, a process known as radiometric determination.

(4) Study area image clip

The downloaded image data is relatively regular and covers a large area, after conductions of Atmospheric correction, Radiometric calibration, and other processes, remote sensing dataset should be clipped into imaged in demand.

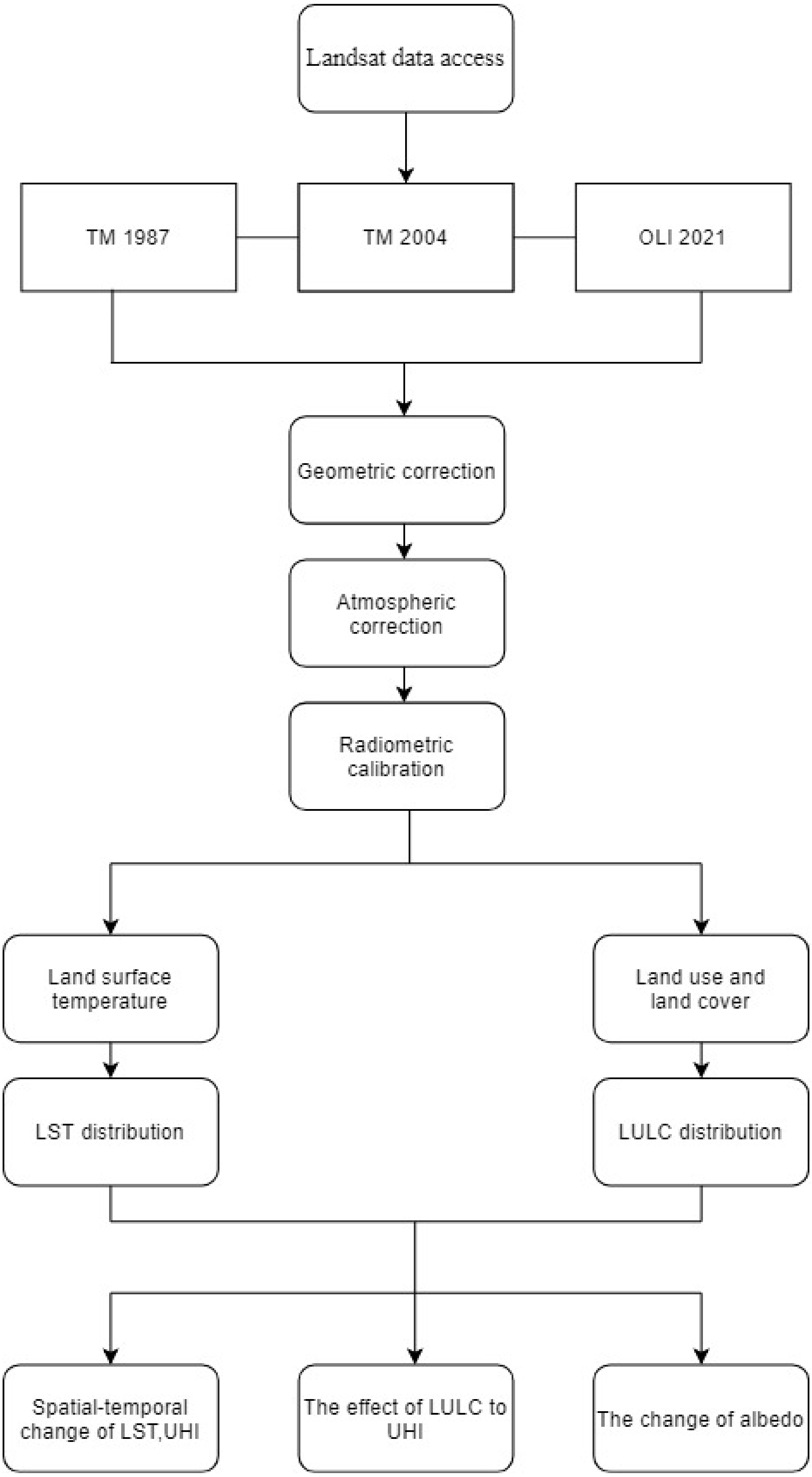

Figure 3: the flowchart of the Technical Route.

2. Supervised Classification

We created training samples and use the maximum likelihood method to classify each Landsat image into 4 classes, they are urban area, water area, barren area, and forest area.

2.1 Accuracy Assessment

The accuracy of the categorized pictures, which is essential for supervised classification, will be assessed using the Confusion matrix approach. The following equation will be used to determine the global, user, and producer accuracy.

2.2 land surface temperature (LST)

The surface temperature determined by satellite thermal bands has previously undergone radiometric and geometric corrections. For this study, the surface temperature was determined using the thermal bands of Landsat 5 and Landsat 8. Landsat 5 has just one thermal band (band 6), but Landsat 8 has two (bands 10 and 11), however band 11 was not utilized for LST calculation due to major calibration issues uncovered by the USGS. Digital number (DN) is the thermal band that Landsat acquires. Consequently, we must translate the DN values into surface temperature.

In this investigation, Landsat thermal bands were processed using the method outlined by Artis and Carnahan (1982). In the first step, the DN values were converted to spectral radiance, and surface temperature was then created from spectral radiance in the second.

In Landsat 5 and Landsat 8, DN values are converted differently to radiance. The following equation [46] describes the transformation of Landsat 5 TM DN values to spectral radiance. The terms *LMAXλ* and *LMINλ* refer to the maximum and minimum radiances, respectively. *QCALMAX* and *QCALMIN* refer to the quantized maximum and minimum, respectively.

Lλ represents spectral radiance, while QCAL represents thermal band 6. The thermal band of Landsat 5 TM is band 6, and values can be obtained from the image's metadata file. The equation describes how Landsat 8 converts DN to spectral radiance.

In Landsat 8, the thermal band corresponds to band 10, whereas ML stands for Multiplicative band 10, QCAL for Thermal band 10, and AL for Additive band 10.

$$T = K2 / Ln\left(\frac{K1}{L\lambda} + 1\right) - 273.15 \qquad (8)$$

Using an equation, the spectral radiance was converted to the temperature of the surface in degrees Celsius. K1 and K2 are constant integers discovered within the metadata file. Lλ stands for spectral radiance, while T refers to temperature.

$$LST = \frac{T}{1 + \left(\lambda * \frac{T}{\rho}\right) * In(\varepsilon)} \qquad (9)$$

Land surface temperature (LST), where T is computed as the degree of satellite brightness. The wavelengths of Landsat 5 TM Band 6 (11.5 m) and Landsat 8 OLI Band 10 (10.8 m) are measured in degrees Celsius. The equation is utilized to calculate the emissivity (ε) of the land surface.

$$\varepsilon = 0.004 * \mathrm{P}_v + 0.986 \qquad (10)$$

Calculated using NDVI readings, the percentage of vegetation (Pv). As a result, we first computed the NDVI (Equation) before utilizing the equation to determine the amount of vegetation.

$$NDVI = \frac{NIR - RED}{NIR + RED} \qquad (11)$$

$$P_v = \left(\frac{NDVI - NDVI_{min}}{NDVI_{max} - NDVI_{min}} \right)^2 \qquad (12)$$

3. Correlation between LST and EDVI, NDBI

NDVI: In comparison to other wavelengths, thriving vegetation (chlorophyll) reflects greener and near-infrared light. However, bluer, and red radiation is absorbed. The result of this equation is a number between -1 and 1. Consequently, the NDVI will be high if the red channel has low reflectance (or low values) and the NIR channel has high reflectance. And vice versa. NDVI is a standard method for measuring the condition of vegetation.

$$NDVI = \frac{NIR - RED}{NIR + RED} \qquad (13)$$

NDBI: Normalized Differential Building-up Index is one of the most widely used indexes to enhance the display of building information and to extract building land. The formula is as follows:

$$NDBI = \frac{(SWIR - NIR)}{(SWIR + NIR)} \quad (14)$$

4. UHII

In this investigation, the simplified urban extent (SUE) algorithm was used to determine the SUHI. The calculation methods for the SUHI are provided below. From the extracted LULC data, we constructed two subsets: one for urban area and one for LULC classes excluding urban area and aquatic bodies. Water may exaggerate or underestimate the SUHI during the day and at night because of its high heat capacity. After computing the LST for urban and non-urban regions, the SUHI was created by dividing the mean LST of urban and non-urban areas.

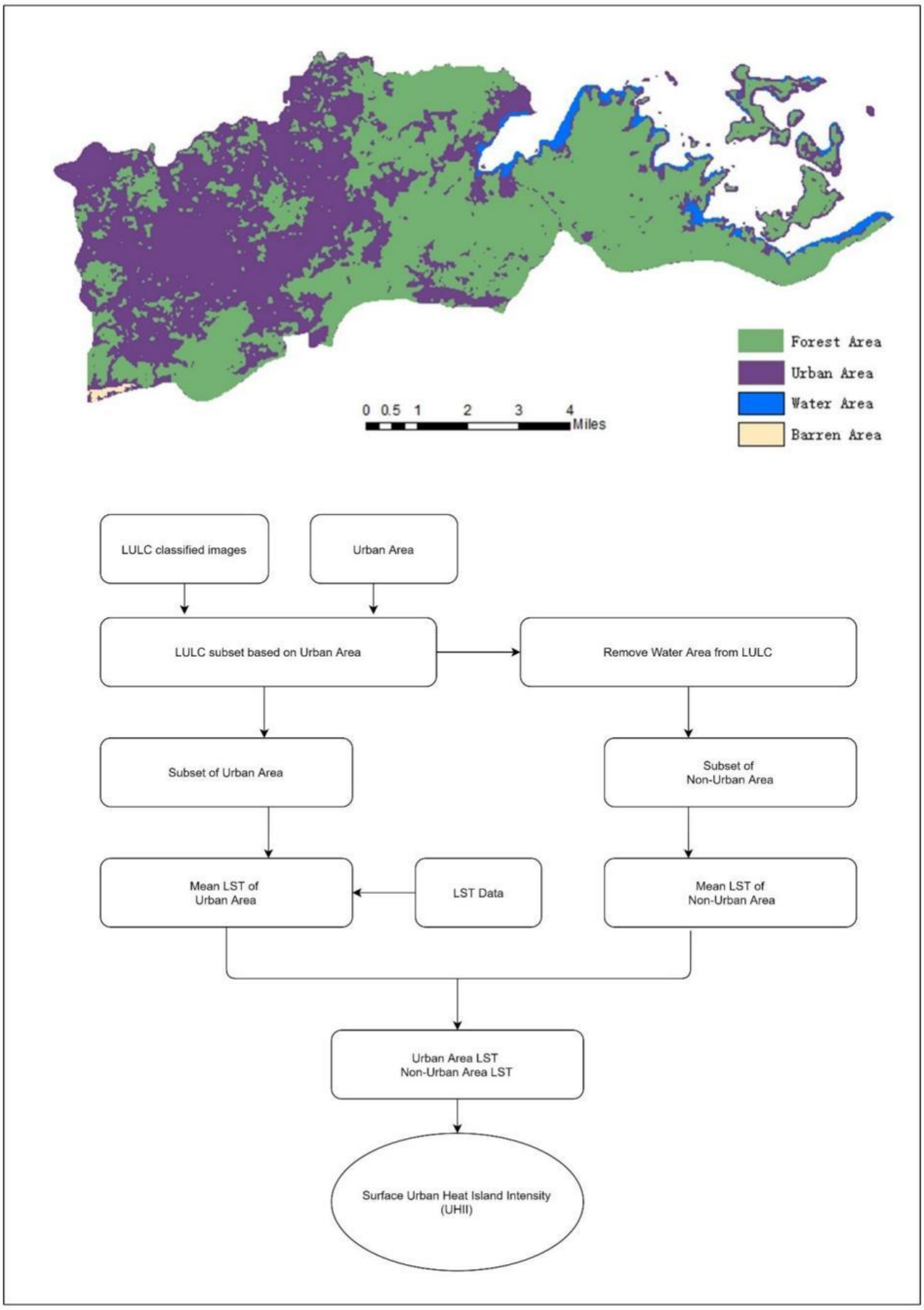

Figure 4: Urban heat island intensity flow chat

CHAPTER IV. OUTCOME

After classifying LULC utilizing supervised classification (maximum likelihood method), the classified images are divided into four categories: Water area, Forest area, Urban area, and Barren area, and then, analyze LULC change in north district of Hong Kong, we associate LULC with land surface temperature (LST), calculate the surface urban heat island intensity (SUHI), we discover a correlation between LULC change and LST, allowing us to determine the effect of urbanization on the urban heat island.

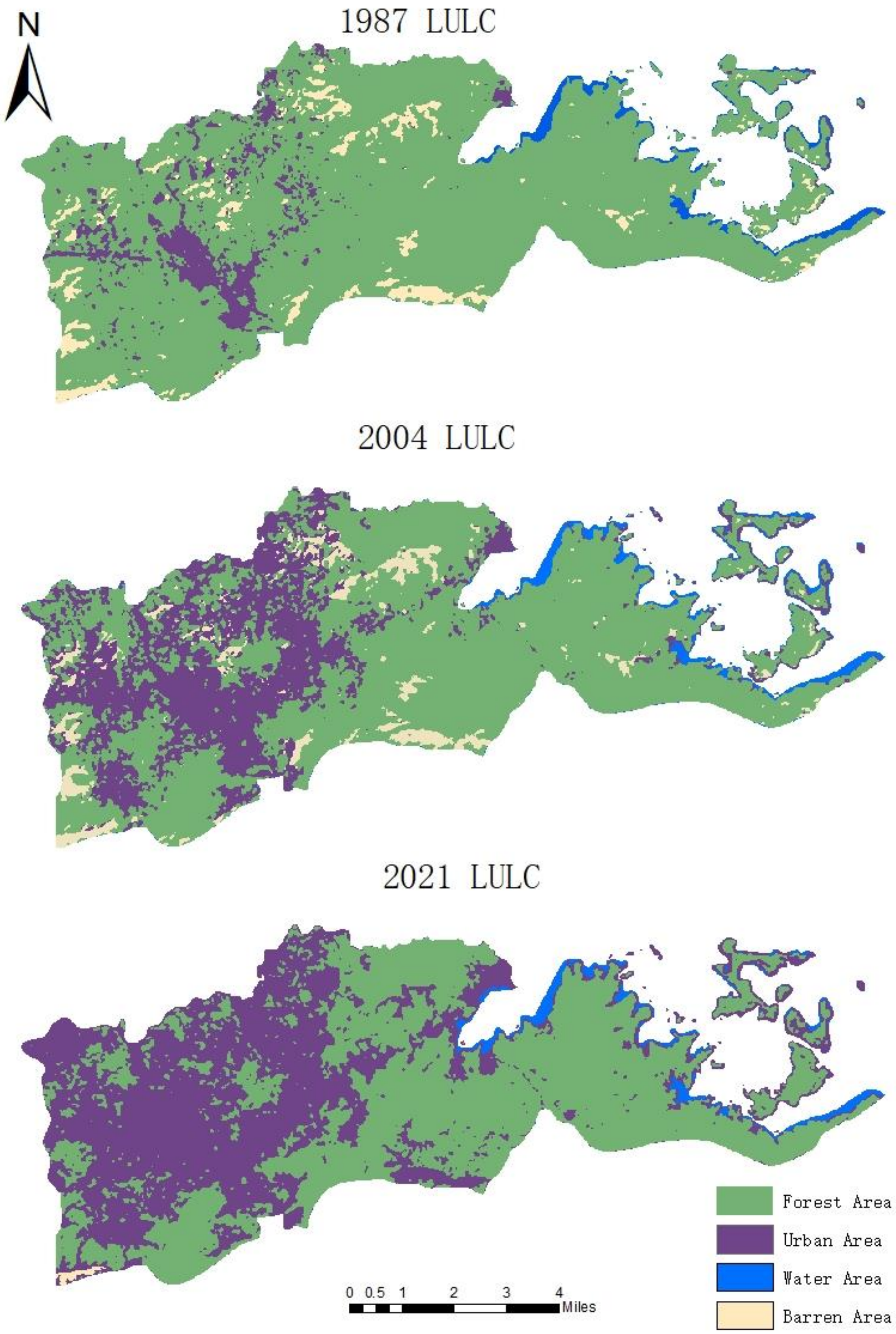

Figure 5: LULC classification result

1. Separability

The separability between classes can reflect the selection of regions of interests (ROIs) quality before classification, we can see, in this study, the separability between forest area and urban area, forest area and barren area, urban area and barren area among 1987,2004, and 2021 are more than 1.9, and the separability between water area and barren area is 2.0, that means the quality of ROI is much high.

Table 3: Separability of supervised classification

CLASS \ TIME	1987	2004	2021
Forest area - Urban area	1.95160	1.95285	1.99419
Forest area - Barren area	1.97296	1.99240	1.99959
Urban area - Barren area	1.99138	1.99287	1.99990
Forest area - Water area	1.99828	1.99327	2.00000
Water area - Urban area	2.00000	2.00000	2.00000
Water area - Barren area	2.00000	2.00000	2.00000

2. Accuracy evaluation of LULC

Using the error matrix, the accuracy evaluation (kappa coefficient and overall accuracy) is generated for all classified images. For the years 1987, 2004 and 2021, respectively, the aggregate accuracy was greater than 99%, 96%, and 99%. While kappa co-efficient was above 0.99,0.94, and 0.99 for the years of 1987, 2004, and 2021.the overall accuracy and kappa coefficient are much high, it proves that the quality of classification is excellent.

Table 4: LULC classification accuracy

	1987	2004	2021
Overall Accuracy	99.80%	96.77%	99.49%
Kappa Coefficient	0.9960	0.9401	0.9922

3. Land use and land cover (LULC) classification result

According to classification outcomes, from 1987 to 2004, 71.157% of forest area remained unchanged, 26.903% of forest were changed into urban area, 9.529% of barren area were changed into urban area. From 2004 to 2021, 71.157% of forest area remained unchanged, 26.903% of forest area were changed into urban area, 9.529% of barren area were changed into urban area. From 1987 to 2021, 42.654% of forest area changed into other land areas. 42.177% of the forest was converted into urban area. From 1987 to 2021, forested land was converted to urban land, and urbanization continued to expand.

Table 5: Land-use transfer matrix

1987 \ 2004	1987 to 2004 Land-use transfer matrix - percentage (%)				
	Forest area	Urban area	Water area	Barren area	Class Total
Forest area	71.157	26.903	0.525	1.415	100
Urban area	0	99.902	0	0.098	100
Water area	0.211	0.702	99.052	0.035	100
Barren area	8.811	9.529	0.081	81.579	100
Class Total	100	100	100	100	0

2004 \ 2021	2004 to 2021 Land-use transfer matrix - percentage (%)				
	Forest area	Urban area	Water area	Barren area	Class Total
Forest area	76.505	23.159	0.333	0.003	100
Urban area	8.064	91.505	0.428	0.002	100
Water area	0.638	51.446	47.916	0	100
Barren area	36.958	59.6	0	3.442	100
Class Total	100	100	100	100	0

1987 \ 2021	1987 to 2021 Land-use transfer matrix - percentage (%)				
	Forest area	Urban area	Water area	Barren area	Class Total
Forest area	57.346	42.177	0.468	0.009	100
Urban area	3.082	96.918	0	0	100
Water area	0.176	48.35	51.474	0	100
Barren area	36.853	59.604	0	3.543	100
Class Total	100	100	100	100	0

4. Calculation of NDVI and FVC through ENVI 5.3

A negative number denotes a ground cover that reflects more visible light, such as clouds, precipitation, snow, etc., whereas a positive value denotes a ground cover that reflects less visible light, such as vegetation. 0 indicates rock or barren soil, and NIR and Rare are roughly equivalent. NDVI can reflect the underlying influences of a plant canopy, such as soil, moisture, precipitation, and decomposition. vegetation cover is correlated with foliage, texture, etc. We calculated NDVI using ENVI 5.3 and obtained the NDVI graph, which can also reflect the degree of urbanization.

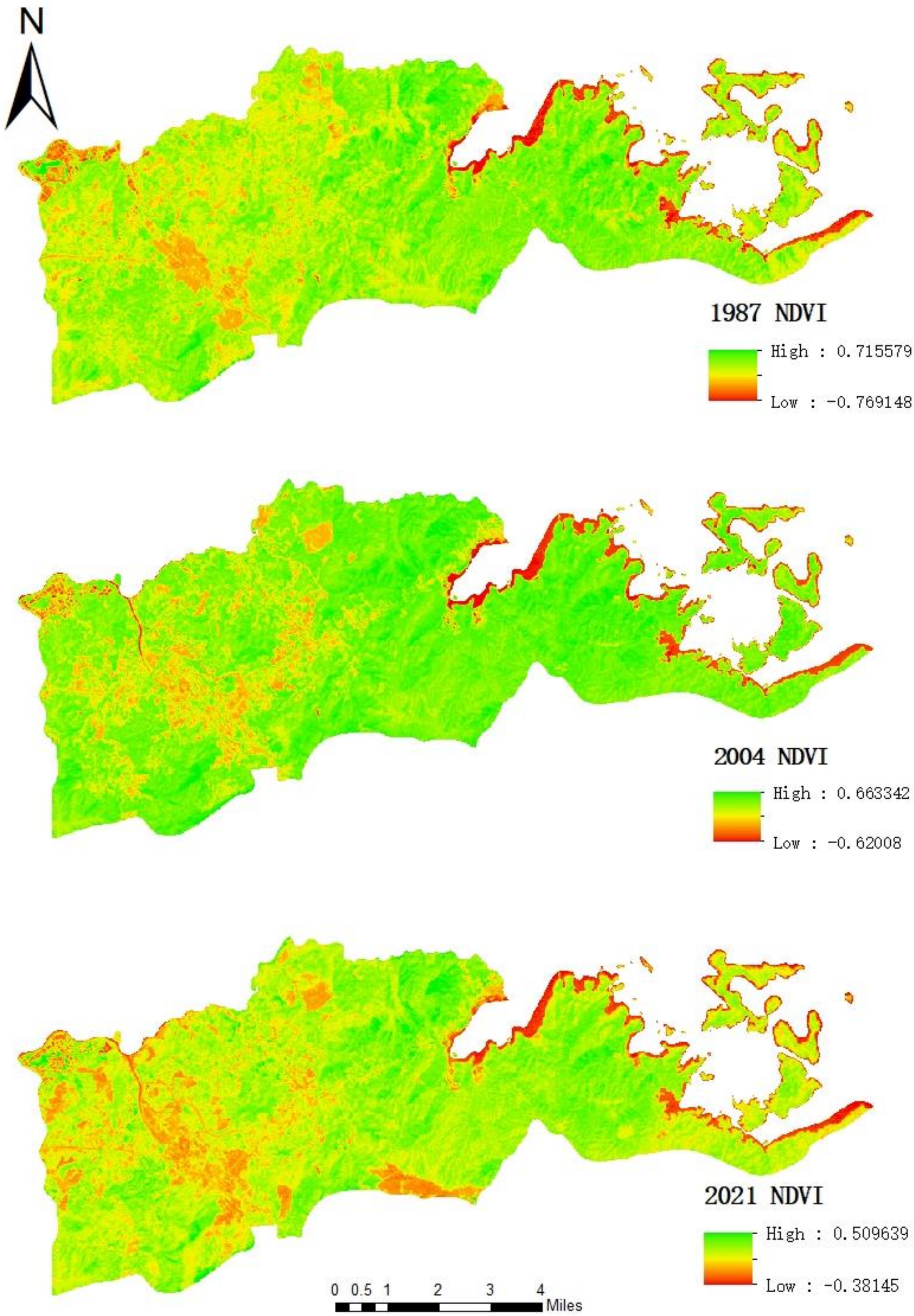

Figure 6: NDVI of north district of Hong Kong

As an essential component of the ecological cycle, vegetation plays a crucial role in the global energy and material cycles. Fractional vegetation cover (FVC) is typically used to describe the surface vegetation cover and is the ratio of the vertical projection area of the ground's plant canopy to the overall area of the land.

5. Correlation analysis between UHI and NDVI and NDBI

In 1987, NDVI and LST had a correlation value of -0.61274; NDBI and LST had a correlation coefficient of 0.59873; in 2004, NDVI and LST had a correlation coefficient of -0.48521; and in 2021, NDVI and LST had a correlation coefficient of -0.40626; NDBI and LST had a correlation coefficient of 0.77621.

Table 6: The relationship between LST and NDVI

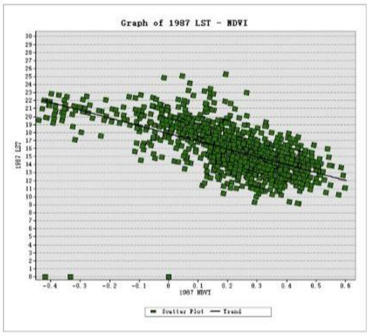

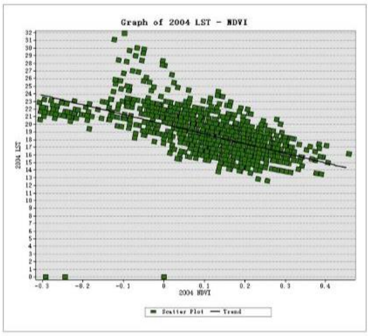

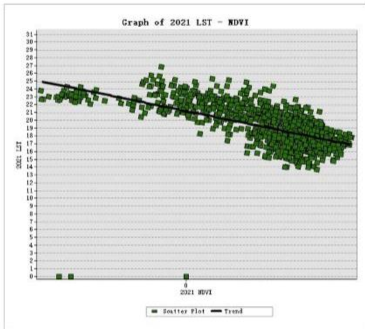

Table 7: The correlation between LST and NDBI

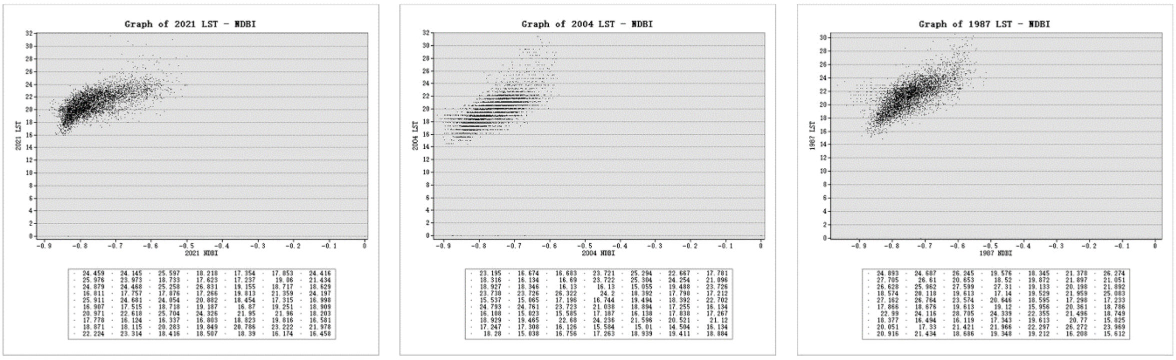

6. Relationship between LST and LULC

This investigation measured the land surface temperature (LST) in the Hong Kong North district using the Landsat thermal band. Landsat 5 TM images from December 1987, Landsat 5 TM images from December 2004 and Landsat 8 images from December 2021 were acquired. We can observe a spatial increase in LST in the study area, and the LST distribution is comparable to the LULC map. In 1987, high LST in the study area was primarily distributed in urban and desolate areas, whereas the high temperature distribution range was not the same; however, in 2004 a much greater proportion of the study area encountered high temperatures in urban and desolate areas. Due to urbanization, the north district of Hong Kong will become harsher in 2021, with temperatures reaching above 30 degrees Celsius. The decreased temperature in the study's eastern region is a result of the forest and aquatic regions. The variations in LST reflected the effect of land change. Continuous urban area expansion and a rise in LST suggest that urbanization has an impact on LST. Observing the land surface temperature (LST) between our research and the satellite transit time LST is challenging. So we used 0 cm Ground Temperature from National Meteorological Information Center of Hong Kong for comparison. After comparison, I found the error between our study and meteorological observatory observation data is under 2.0 °C, based on our purpose of study, the error is within a reasonable range, it can meet the needs of study.

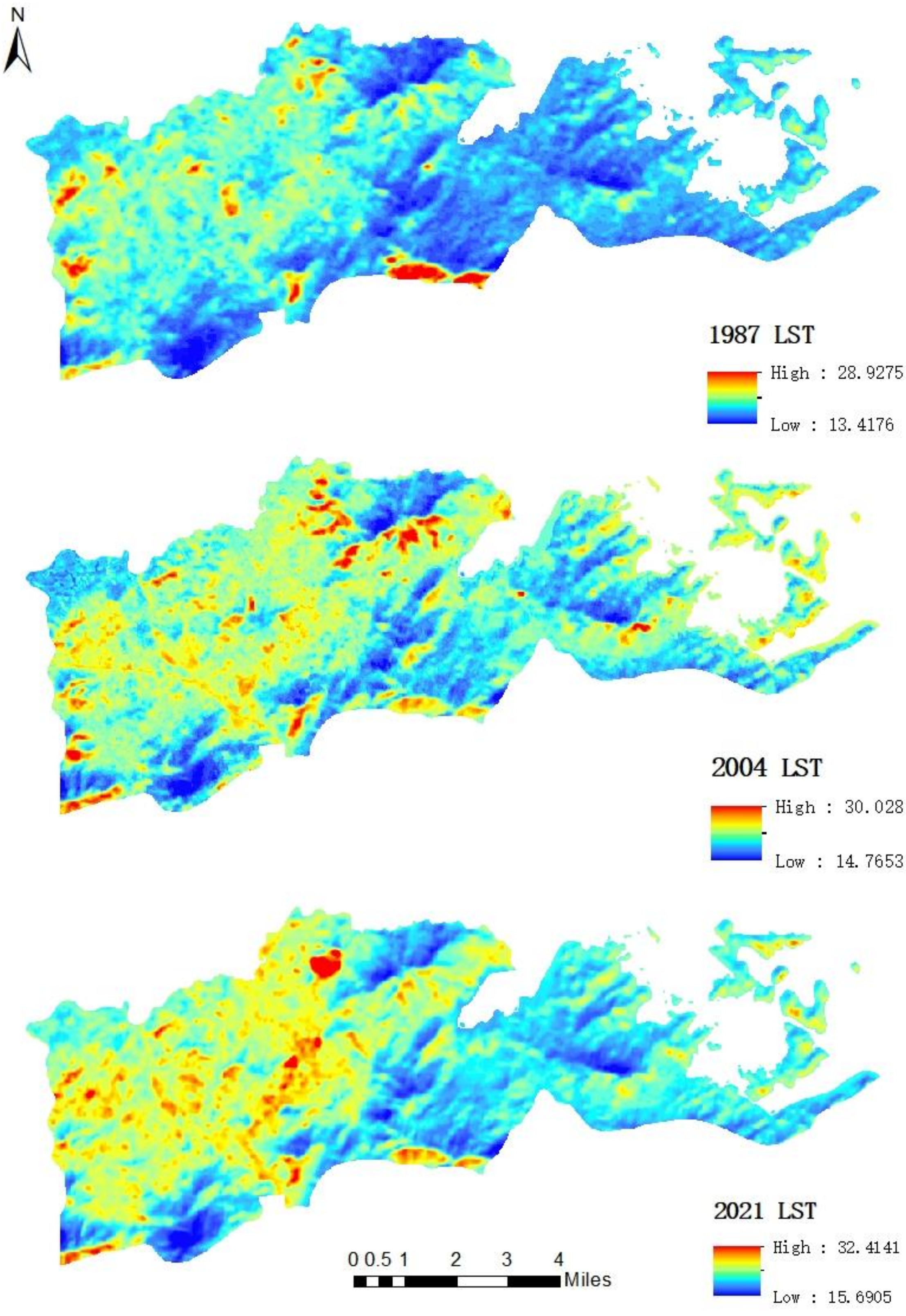

Figure 7: Land Surface Temperature of North District of Hong Kong

According to the research of Muhammad Farhan Ul Moazzam, urban areas significantly contribute to the rise in LST, and changes in land use and land cover (LULC) may have a negative impact on the geographical distribution of land surface temperature (LST) there, in 1987, when the urban area was 13.56% of the portion in North district of Hong Kong, the average temperature was 17.67 °C, but when the urban area reached 51.32% in 2004, it rose to 20.30 °C, in 2021, the urban area was 62.34% and the mean temperature was 24.74°C, shown that urbanization directly affects LST. Fig. 8 demonstrated the connection between urban areas and LST.

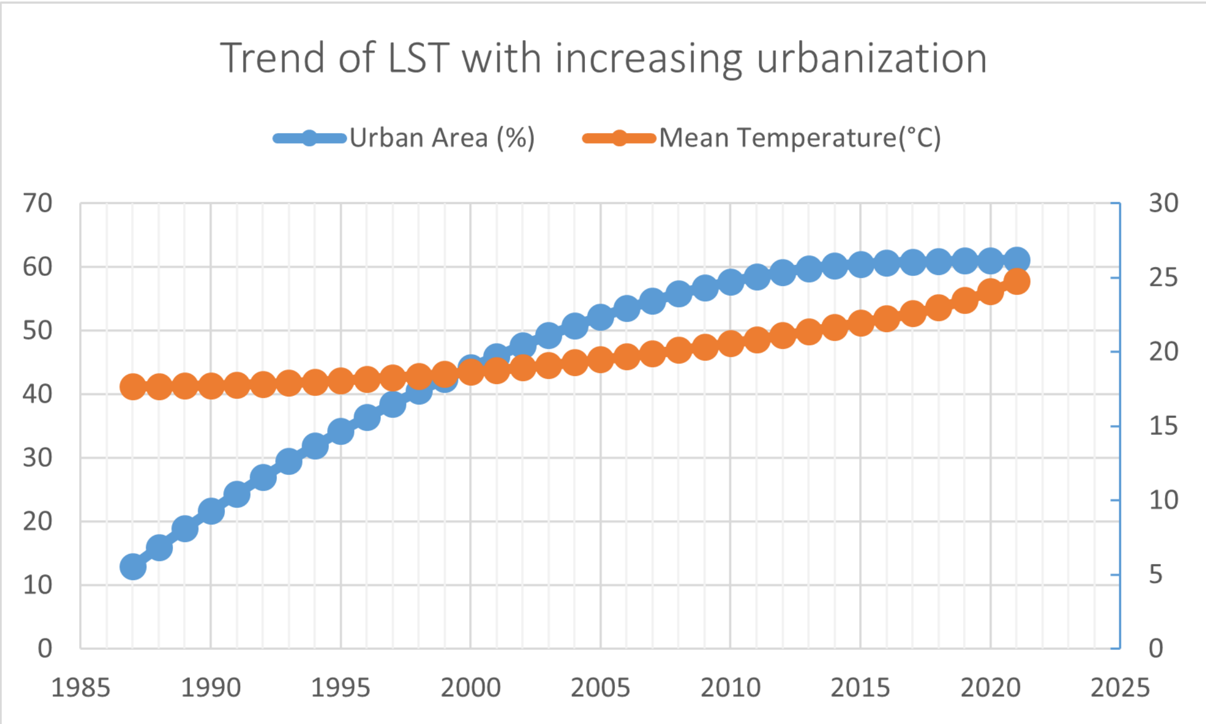

Figure 8: Trend of LST with increasing urbanization.

7. The Albedo and LST

From the albedo map, it shows that the distribution of albedo change is the same with the LULC change, as the urbanization and urban growth take place in north district of Hong Kong, the surface of this region changes at the same time, especially, the impervious surface and forest area surface, all these changes take place with the albedo change by the same time. The result shows that the distribution of LULC, albedo and LST is the same.

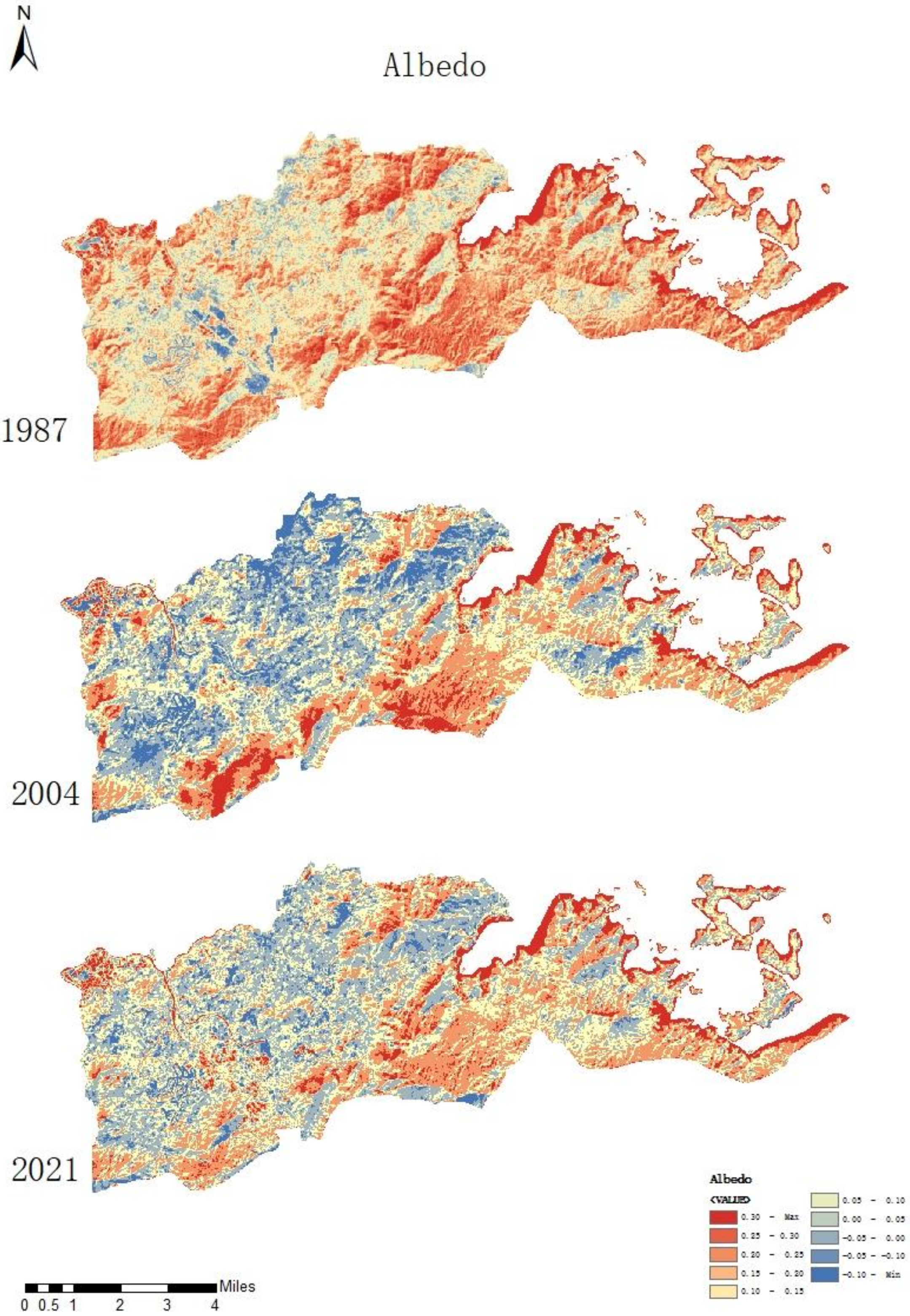

Figure 9: The distribution of albedo in North District of Hong Kong.

8. Analysis of Albedo and LST in significant sub-areas

The cyan-red scale images below clearly demonstrate the direct relationship between the surface albedo and the LST values of the building's interesting regions. Images of Δα and LST demonstrate the clear relationship between surface albedo and LST values of interest regions. As pictures 1,2,3,4, shown, there are no changes in these regions from 1987 to 2021. However, in pictures 5,6,7,8, the surfaces of these regions changed. In picture 6, the surface albedo diminished strongly with 0.13, resulting in a temperature increase of 4.7 °C.

In the southeast of Hong Kong's north district, many residential areas had solar roofs. As shown in image 8, the photovoltaic roof led to a 0.09 reduction in albedo and a 5.8 °C rise in LST as a result.

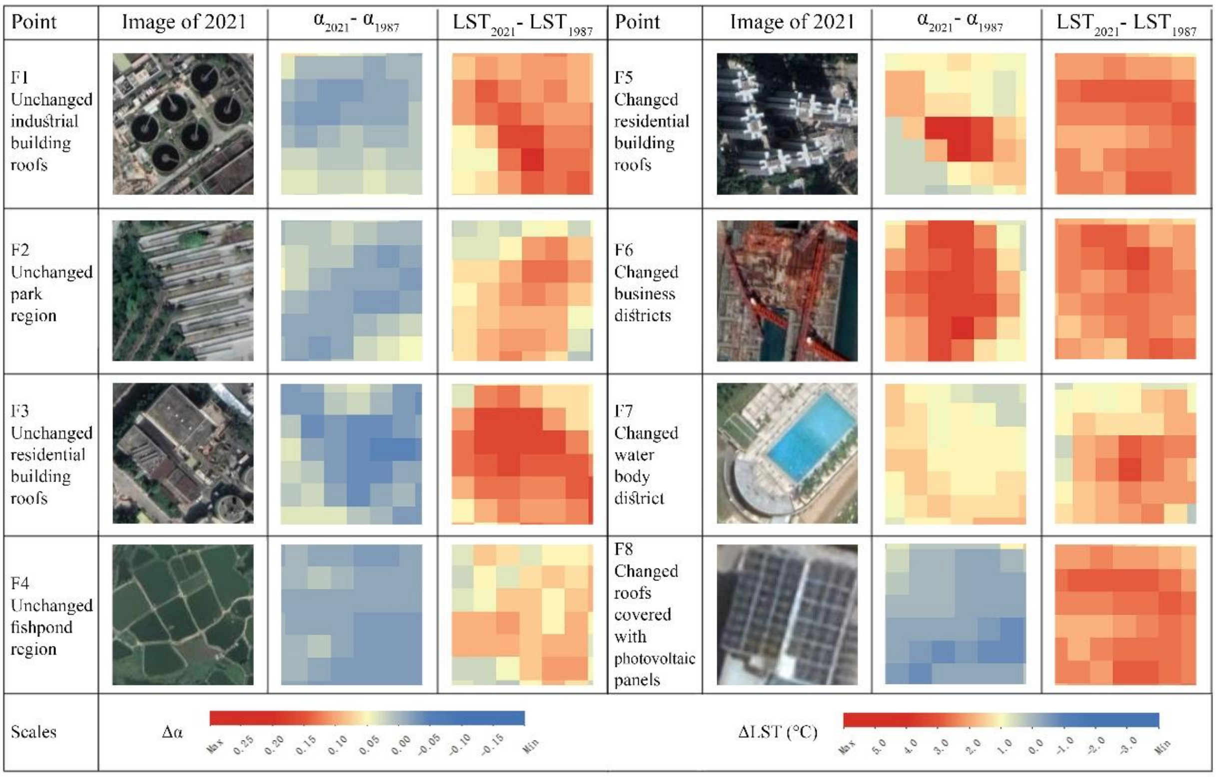

Figure 10: Albedo and LST in significant sub-areas.

9. The distribution of SUHI in the North District of Hong Kong

Urban heat island surface intensity (SUHI) has been determined. According to the findings, the metropolitan area's average surface temperature in the North District of Hong Kong was 17.6724 °C in 1987, rose to 20.2954 °C in 2004, then rose to 22.9465 °C by 2021. In 1987, the non-urban LST was 8.4176 °C; in 2004, it was increased to 10.7653 °C; and in 2021, it was raised once more to 11.6905 °C. Surface urban heat island, or SUHI, is the difference between the mean surface temperature of an urban area and an undeveloped area. For three years, SUHI was computed. In 1987, there was a difference in mean LST between urban and non-urban area of 8.2548 °C; this value grew to 10.5304 °C and 11.2565 °C in 2004 and 2021, respectively.

10.the development of urbanization and urban heat island in the North District of Hong Kong.

According to literature review research, the findings demonstrated a favorable association between urban heat island and urban area land use and land cover (LULC), and the association between urban heat island and water area, forest area is negative. In this study, the land use and land cover (LULC) results show that the expansion of urban area could increase the land surface temperature (LST), whereas the urban heat island intensity is the temperature difference between urban and non-urban areas. So, the urbanization speed goes faster, the land surface temperature of the urban area increases faster, and the surface urban heat island more serious.

in 1987, when the urban area was 13.56% of the portion in the North district of Hong Kong, when the urban area reached 51.32 percent in 2004, the average temperature was 17.67 °C and rose to 20.30 °C, in 2021,the urban area was 62.34% and the mean temperature was 24.74°C, in 1987, there was an 8.2548 °C difference between the mean LST of urban and non-urban areas, but it grew to 10.5304 °C and 11.2565 °C in 2004 and 2021 [67,68,69].

CHAPTER V. CONCLUSION

To investigate how urbanization and the surface urban heat island are related, i categorized Landsat 5, Landsat 8, and LULC pictures by using maximum likelihood supervised classification. The separability of supervised classification is sufficient, and the Kappa coefficient and overall accuracy range from 96% to 99%, or from 0.94 to 0.99, respectively. In the result of LULC classification, I got the land-use transfer matrix of the North district of Hong Kong, from 1987 to 2004, 71.157% of forest area was retained, 26.903% of forest was changed into urban area, 9.529% of barren area was changed into urban area. From 2004 to 2021, 71.157% of forest area was retained, 26.903% of forest area was changed into urban area, and 9.529% of barren area was changed into urban area. 42.654% of the forestland was converted to other land uses between 1987 and 2021, while 42.177% of the forestland was converted to urban space. From 1987 to 2021, forest land was converted to urban land, and this urbanization trend persisted.

Then I got the inversion LST based on the radiation transfer equation method through the thermal band of Landsat 5/ Landsat 8 images in ENVI 5.3, I can find that the distribution of high temperature is basically the same as urban area and barren area in LST maps and LULC maps. Surface urban heat island (SUHI) may be estimated by comparing the mean surface temperatures of urban and non-urban areas. In the North District of Hong Kong, the SUHI for 1987, 2004, and 2021 was determined. In 1987, there was an 8.2548 °C difference between the mean LST of urban and non-urban areas, but it grew to 10.5304 °C and 11.2565 °C in 2004 and 2021, respectively. I have hypothesized that the North District of Hong Kong's high surface temperature is caused by urban growth, which implies there is a direct correlation between urban growth and LST and it is the primary source of the LST increase. In this investigation, it was also shown that the SUHI intensity rose by 2.0017 °C between 1987 and 2021.

On the other hand, I have examined the correlation trend between the LST and EDVI, and NDBI to determine the correlation trend between the LST distribution and urban building land and green space. According to the correlation coefficients between NDVI and LST, which are -0.61274 in 1987, -0.48521 in 2004, -0.70397 in 2021, and -0.40626 in 2021, urban heat islands are negatively impacted by urban green space. Urban building land has a positive impact on the urban heat island, which suggests that urban building land may boost the urban heat island effect, according to the positive association between urban building land and surface temperature distribution. Hence, the North District of Hong Kong has suffered significantly as a result of urbanization, which is also to blame for the region's rising temperatures.

Main innovations and limitations in this study

Innovations:1. The combination of land use and land cover (LULC) and the inversion of Land surface temperature (LST) make the relationship between urbanization and urban heat island effect clearer.2. I selected Albedo and LST in significant sub-areas, the analysis of interesting points can reveal the change of albedo of North District of Hong Kong as time goes by in different regions.

Limitations:1. In this study, I used the winter dataset to get the winter urban heat island, but without the summer urban heat island. 2. I just got the urban heat island development and situation of the North District of Hong Kong, however, the climate in Hong Kong is complex and multivariate, Studying the whole Hong Kong urban heat island effect is more serious than part of Hong Kong city.

Research prospect of urban heat island in Hong Kong region

This study used 3 datasets to get the urban heat island development and situation in the North District of Hong Kong. I analyzed the land use and land cover (LULC) change and the impact on land surface temperature (LST) and urban heat island, then, revealed the relationship between urbanization and urban heat island, however, the dataset is limited, and the result is just winter urban heat island, and the research range is just North District of Hong Kong but not the whole Hong Kong city. The relationship between urbanization and urban heat island is just surface urban heat island, the result can just reveal the urban heat island effect in the North District of Hong Kong through a two-dimensional surface aspect, in the future, the study should take urban form into account to research urban heat island in Hong Kong from three-dimensional space.

REFERENCE

1. Ayanlade, A. (2016). Seasonality in the daytime and night-time intensity of land surface temperature in a tropical city area. Science of the Total Environment, 557, 415-424.

2. Ben Dong, Shuyi Dong, Yingchun Wang, Fayang Wen, Chunmei Yu, Jinlin Zhou, Rongcai Song. "Detecting Geothermal Resources in a Plateau Area: Constraints From Land Surface Temperature Characteristics Using Landsat 8 Data", Frontiers in Earth Science, 2022.

3. Dan Meng, Huili Gong, Xiaojuan Li, Wenji Zhao, Zhaoning Gong, Lin Zhu, Deyong Hu. "Study of thermal environment based on remote sensing in Beijing-capital zone", 2009 IEEE International Geoscience and Remote Sensing techlologe.

4. Dilawar, A., Chen, B., Trisurat, Y., Tuankrua, V., Arshad, A., Hussain, Y., ... & Sun, S. (2021). Spatiotemporal shifts in thermal climate in responses to urban cover changes: a-case analysis of major cities in Punjab, Pakistan. Geomatics, Natural Hazards and Risk, 12(1), 763-793.

5. Elfert, S.. "Simulated impact of past and possible future land use changes on the hydrological response of the Northern German lowland 'Hunte' catchment", Journal of Hydrology, 20100330.

6. Ellis, P., & Roberts, M. (2015). Leveraging urbanization in South Asia: Managing spatial transformation for prosperity and livability. World Bank Publications.

7. Faqe Ibrahim, G. R. (2017). Urban land use land cover changes and their effect on land surface temperature: Case study using Dohuk City in the

Kurdistan Region of Iraq. Climate, 5(1), 13.Fei Zhang, Hsiangte Kung, Verner Carl Johnson, Bethany Iris LaGrone, Juan Wang. "Change Detection of Land Surface Temperature (LST) and some Related Parameters Using Landsat Image: a Case Study of the Ebinur Lake Watershed, Xinjiang, China", Wetlands, 2017.

8. "Geospatial Data Analytics and Urban Applications", Springer Science and Business Media LLC, 2022.

9. Guanghao Li, Zhihui Ren, Changhong Zhan. "Sky View Factor-based correlation of landscape morphology and the thermal environment of street canyons: A case study of Harbin, China", Building and Environment, 2020.

10. Heat Island Effect over Jinan City Using the Markov- Cellular Automata Model Combined with Urban Biophysical Descriptors", Journal of the Indian Society of Remote Sensing, 2021.

11. He, Z., Gao, Y., Bai, Y., & Yang, S. (2010, May). Monitoring and simulating urban heat island phenomenon during unusual high temperature and drought period in 2006 summer in Chongqing, China. In 2010 Second International Conference on Modeling, Simulation and Visualization Methods (pp. 70-73). IEEE.

12. Hongli Song, , Xiaonan Zhang, and Haixin Liu. "Observation of thermal space environment based on remote sensing", 2011 International Conference on Remote Sensing Environment and Transportation Engineering, 2011.

13. Hongrui Wen, Qiaozhen Guo, Yuhuai Zeng, Zepeng Wu, Zhenhui Sun. "Study on forest fire risk in Conghua district of Guangzhou city based on multi-source data", Natural Hazards, 2022.

14. HOWARD L. Climate of London Deduced from Metrological Observations.

London: Harvey and Dorton Press, 1833.

15. Hu, X. M., & Xue, M. (2016). Influence of synoptic sea-breeze fronts on the urban heat island intensity in Dallas–Fort Worth, Texas. Monthly Weather Review, 144(4), 1487-1507.

16. Iain D. Steward Gerald Mills.The urban heat island a guidebook.

17. Imran, M., & Mehmood, A. (2020). Analysis and mapping of present and future drivers of local urban climate using remote sensing: a case of Lahore, Pakistan. Arabian Journal of Geosciences, 13, 1-14.

18. Jae-Dong Jang. "Thermal-water stress index from satellite images", International Journal of Remote Sensing, 4/1/2006.

19. Jérémy Bernard, Marjorie Musy, Isabelle Calmet, Erwan Bocher, Pascal Keravec. "Urban heat island temporal and spatial variations: Empirical modeling from geographical and meteorological data", Building and Environment, 2017.

20. Jiansheng Wu, Chang Liu, Hongliang Wang. "Analysis of Spatio-temporal patterns and related factors of thermal comfort in subtropical coastal cities based on local climate zones", Building and Environment, 2021.

21. Juro HANYU, Seiichi SANO, Shoichiro YAMANAKA, Daizo IGARASHI, Shigehisa SUGIYAMA. "A Simple Frost-damage Box Utilizing Natural Radiative Cooling", Journal of Agricultural Meteorology, 1979.

22. Kafy, A. A., Rahman, M. S., Hasan, M. M., & Islam, M. (2020). Modelling future land use land cover changes and their impacts on land surface temperatures in Rajshahi, Bangladesh. Remote Sensing Applications: Society and Environment, 18, 100314.

23. Kim, Y. H., & Baik, J. J. (2004). Daily maximum urban heat island intensity in large cities of Korea. Theoretical and Applied Climatology, 79, 151-164.

24. Lei Wang. "Study on Evolvement of Urban Thermal Environment Spatial Patterns Based on RS and GIS -- a Case Study of Changchun City, Jili Province, China", 2011 Fourth International Symposium on Knowledge Acquisition and Modeling, 10/2011.

25. Li Juan Zhang, Xing Ping Wen, Jun Wang, Yang Zhou. "Research on the Relationship of Surface Temperature and Urban Heat Island Using the Thermal Infrared Remote Sensing Image", Advanced Materials Research, 2014.

26. Liu, H., Tu, G., & Dong, W. (2008). Three-year changes of surface albedo of degraded grassland and cropland surfaces in a semiarid area. Chinese Science Bulletin, 53(8), 1246-1254.

27. Liu, Lin, and Yuanzhi Zhang. "Urban Heat Island Analysis Using the Landsat TM Data and ASTER Data: A Case Study in Hong Kong", Remote Sensing, 2011.

28. Liu, W., Ji, C., Zhong, J., Jiang, X., & Zheng, Z. (2007). Temporal characteristics of the Beijing urban heat island. Theoretical and Applied Climatology, 87, 213-221.

29. LI Zhaoliang, DUAN Sibo, TANG Bohui, WU Hua, REN Huazhong, YAN Guangjian, TANG Ronglin, LENG Pei. 2016. Review of methods for land surface temperature derived from thermal infrared remotely sensed data.Journal of Remote Sensing, 20(5): 899-920.

30. Manley, G. (1958). On the frequency of snowfall in metropolitan England. Quarterly Journal of the Royal Meteorological Society, 84(359), 70-72.

31. Mell, I. (2016). Global green infrastructure: lessons for successful policy-making, investment and management. Routledge.

32. Meng, X., Meng, F., Zhao, Z., & Yin, C. (2021). Prediction of urban heat island effect over Jinan City using the markov-cellular automata model combined with urban biophysical descriptors. Journal of the Indian Society of Remote Sensing, 49, 997-1009.

33. Muhammad Farhan Ul Moazzam, Yang Hoi Doh, Byung Gul Lee. "Impact of urbanization on land surface temperature and surface urban heat Island using optical remote sensing data: A case study of Jeju Island, Republic of Korea", Building and Environment, 2022.

34. Oke T R. Boundary layer climate [M]. Cambridge: Great Britain at the University Press, 1987: 1-3.

35. Prashanthini Rajagopal, Radhakrishnan Shanthi Priya, Ramalingam Senthil. "A review of recent developments in the impact of environmental measures on urban heat island", Sustainable Cities and Society, 2022.

36. Priyadarsini, R., Hien, W. N., & David, C. K. W. (2008). Microclimatic modeling of the urban thermal environment of Singapore to mitigate urban heat island. Solar energy, 82(8), 727-745.

37. Rehan, R. M. (2016). Cool city as a sustainable example of heat island management case study of the coolest city in the world. HBRC journal, 12(2), 191-204.

38. Renard, F., Alonso, L., Fitts, Y., Hadjiosif, A., & Comby, J. (2019). Evaluation of the effect of urban redevelopment on surface urban heat islands. Remote Sensing, 11(3), 299.

39. Rizvi, S. H., Fatima, H., Alam, K., & Iqbal, M. J. (2021). The surface urban heat island intensity and urban expansion: A comparative analysis for the coastal areas of Pakistan. Environment, Development and Sustainability, 23, 5520-5537.

40. Sajjad Hussain, Muhammad Mubeen, Ashfaq Ahmad, Hamid Majeed et al. "Assessment of land use/land cover changes and its effect on land surface temperature using remote sensing techniques in Southern Punjab, Pakistan", Environmental Science and Pollution Research, 2022.

41. Santamouris, M. (2014). Cooling the cities–a review of reflective and green roof mitigation technologies to fight heat island and improve comfort in urban environments. Solar energy, 103, 682-703.

42. Se Woong Kim, Robert D. Brown. "Urban heat island (UHI) intensity and magnitude estimations: A systematic literature review", Science of The Total Environment, 2021.

43. Shushi Peng, Shilong Piao, Philippe Ciais, Pierre Friedlingstein et al. "Surface Urban Heat Island Across 419 Global Big Cities", Environmental Science & Technology, 2011.

44. Stathopoulou, M., Synnefa, A., Cartalis, C., Santamouris, M., Karlessi, T., & Akbari, H. (2009). A surface heat island study of Athens using high-resolution satellite imagery and measurements of the optical and thermal properties of commonly used building and paving materials. International journal of sustainable energy, 28(1-3), 59-76.

45. Stewart I D, Oke T R.Local climate zones for urban temperature studies Bulletin of the American Meteorological Society, 2012,93(12):1879-1900.

46. Sun Lin, Han Liu-sheng, Wang Yao-ting. "The precise monitoring of Beijing

thermal behaviour", 2009 Joint Urban Remote Sensing Event, 2009.

47. Synnefa, A., Dandou, A., Santamouris, M., Tombrou, M., & Soulakellis, N. (2008). On the use of cool materials as a heat island mitigation strategy. Journal of Applied Meteorology and Climatology, 47(11), 2846-2856.

48. Tang, Y., Shi, T., & Ma, F. (2021, April). Eco-Environmental Effects of Industrial Cities Based on Remote Sensing Images: A Case Study of Shenyang, China. In IOP Conference Series: Earth and Environmental Science (Vol. 719, No. 4, p. 042064). IOP Publishing.

49. Tran, H., Uchihama, D., Ochi, S., & Yasuoka, Y. (2006). Assessment with satellite data of the urban heat island effects in Asian mega cities. International journal of applied Earth observation and Geoinformation, 8(1), 34-48.

50. "Urban Heat Island (UHI) Mitigation", Springer Science and Business Media LLC, 2021.

51. Wang, Y., Berardi, U., & Akbari, H. (2016). Comparing the effects of urban heat island mitigation strategies for Toronto, Canada. Energy and buildings, 114, 2-19.

52. Xiangjin Meng, Fei Meng, Zhan Zhao, Chenglong Yin. "Prediction of Urban Heat Island Effect over Jinan City Using the Markov- Cellular Automata Model Combined with Urban Biophysical Descriptors", Journal of the Indian Society of Remote Sensing, 2021.

53. Xin Zhao, Wanlei Xue, Xiaoyang Lian, Mingqiang Wang, Ying Mu. "Air Conditioning Load Forecasting Model Considering EV and Urban Heat Island Effect", 2022 4th Asia Energy and Electrical Engineering Symposium (AEEES), 2022.

54. Xin Zhao, Wanlei Xue, Xiaoyang Lian, Mingqiang Wang, Ying Mu. "Air Conditioning Load Forecasting Model Considering EV and Urban Heat Island Effect", 2022 4th Asia Energy and Electrical Engineering Symposium (AEEES), 2022.

55. Yang Zhang, Ping Jiang, Hongyan Zhang, Peng Cheng. "Study on Urban Heat Island Intensity Level Identification Based on an Improved Restricted Boltzmann Machine", International Journal of Environmental Research and Public Health, 2018.

56. Yao, Yunjun, Shunlin Liang, and Tongren Xu. "Remote Sensing Data Products for Land Surface Data Assimilation System Application", Land Surface Observation Modeling and Data Assimilation, 2013.

57. Yuejing Gao, Jingyuan Zhao, Li Han. "Exploring the spatial heterogeneity of urban heat island effect and its relationship to block morphology with the geographically weighted regression model", Sustainable Cities and Society, 2022.

58. Zhiyuan Zheng, Zhigang Wei, Zhiping Wen, Wenjie Dong, Zhenchao Li, Xiaohang Wen, Xian Zhu, Dong Ji, Chen Chen, Dongdong Yan. "Inclusion of Solar Elevation Angle in Land Surface Albedo Parameterization Over Bare Soil Surface", Journal of Advances in Modeling Earth Systems, 2017.

59. Zhou Hong-mei, Zhou Cheng-hu, Ge Wei- qiang, Ding Jin-cai. "Spatial distribution characteristics of urban thermal conditions: application of GIS and remote sensing", Journal of Geographical Sciences, 2001.

60. Zhu, J. T., Luo, Y., Zhao, M. X., Wang, L., Gong, C. F., & Liu, Y. S. (2020). Analysing the Growth Condition of Hazel Mushroom Base on the Date of Landsat 8 and the Platform of Envi. The International Archives of the

Photogrammetry, Remote Sensing and Spatial Information Sciences, 42, 953-957.

61. Zian Wang, Qingyan Meng, Mona Allam, Die Hu, Linlin Zhang, Massimo Menenti. "Environmental and anthropogenic drivers of surface urban heat island intensity: A case- study in the Yangtze River Delta, China", Ecological Indicators, 2021.

62. Wang, Ge, and Lin Han. "Progress of Research on Qinghai-Tibet Plateau Satellite Remote Sensing", 2012 2nd International Conference on Remote Sensing Environment and Transportation Engineering, 2012.